Glutathione Interaction with SNS/S Mixed-Ligand Complexes of Oxorhenium(V): Kinetic Aspects and Characterization of the Products

Berthold Nock,[†] Theodosia Maina,[†] Achilleas Tsortos,[†] Maria Pelecanou,[‡] Catherine P. Raptopoulou,[§§] Minas Papadopoulos,[†] Hans-Jürgen Pietzsch,[||] Chariklia I. Stassinopoulou,[‡] Aris Terzis,[§§] Hartmut Spies,[||] Georgios Nounesis,[†] and Efstratios Chiotellis*,[†]

Institute of Radioisotopes−Radiodiagnostic Products, National Centre for Scientific Research "Demokritos", 15310 Ag. Paraskevi, Athens, Greece, Institute of Biology, National Centre for Scientific Research "Demokritos", 15310 Ag. Paraskevi, Athens, Greece, Institute of Materials Science, National Centre for Scientific Research "Demokritos", 15310 Ag. Paraskevi, Athens, Greece, and Institut für Bioanorganische und Radiopharmazeutische Chemie, Forschungszentrum Rossendorf, Postfach 510119, D-0314 Dresden, Germany

Received March 31, 2000

A series of oxorhenium(V) SNS/S mixed-ligand complexes [ReO(L^n/L)] carrying different types of tridentate ligands (L^n) and the same monodentate coligand (L) [L = C_6H_5S, L^1 = $C_2H_5N(CH_2CH_2S)_2$ (**1**), L^2 = $(C_2H_5)_2NCH_2CH_2N(CH_2CH_2S)_2$ (**2**), L^3 = $C_2H_5SCH_2CH_2N(CH_2CH_2S)_2$ (**3**), and L^4 = 2,6-$(SCH_2)_2NC_5H_3$ (**4**)] have been synthesized and characterized by spectroscopic methods and elemental analyses. X-ray structure determination was performed for complexes **3** and **4**. Complex **3** adopts the expected distorted trigonal bipyramidal geometry around the metal in a syn configuration, while complex **4**, due to the aromatic character of the nitrogen of the SNS donor-atom set, exhibits a distorted square pyramidal geometry. The interaction of complexes **1**−**4** with glutathione (GSH) was studied by high-performance liquid chromatography, revealing the rapid formation of the respective daughter complexes **5**−**8**, wherein the L coligand has been substituted by GS. The daughter complexes **5**−**8** have been characterized by ES-MS and 2D NMR spectroscopy. Kinetic aspects of the interaction of complexes **1**−**3** with GSH have been studied by isothermal titration microcalorimetry providing direct measurements of the interaction rate constants as well as of the total enthalpy change. The reaction of complex **1** exhibits the slowest rate and that of complex **2** the fastest. This is in agreement with previously reported trends for analogous ^{99m}Tc complexes.

Introduction

Alterations of regional cerebral blood flow may be reflected in a plethora of cerebrovascular and neurological conditions, such as stroke, epilepsy, or psychiatric disorders. For this purpose, clinical studies of brain perfusion are performed today on a routine basis using SPECT (single-photon emission computed tomography) in combination with either the ^{99m}Tc complex of hexamethylpropylene amine oxime or the ^{99m}Tc-labeled ethylcysteinate dimer. Both compounds are neutral and lipophilic oxotechnetium complexes that cross the intact blood brain barrier by passive diffusion. Their rapid transformation to hydrophilic species in the brain cells provokes their retention in brain tissue, for time sufficient to perform a typical SPECT test employing conventional cameras.[1−4]

Neutral and lipophilic ^{99m}Tc complexes can also be produced upon coordination of an aminedithiolate tridentate ligand and a monothiolate coligand to oxotechnetium. Such mixed-ligand complexes have been thoroughly investigated by us and other groups and have been proposed as agents for the assessment of brain perfusion.[5−9] The results of an extensive structure−activity relationship study including a great number of ^{99m}TcO(SNS/S) complexes revealed that both the substituent on the central nitrogen atom of the SNS ligand and, to a lesser extent, the

* Corresponding author. Tel.: + 301 6513 793. Fax: + 301 6524 480. E-mail: mainathe@mail.demokritos.gr.

[†] Institute of Radioisotopes−Radiodiagnostic Products, National Centre for Scientific Research "Demokritos".

[‡] Institute of Biology, National Centre for Scientific Research "Demokritos".

[§] Institute of Materials Science, National Centre for Scientific Research "Demokritos".

[||] Institut für Bioanorganische und Radiopharmazeutische Chemie, Forschungszentrum Rossendorf.

(1) Neirinckx, R. D.; Canning, L. R.; Piper, I. M.; Nowotnik, D. P.; Pickett, R. D.; Holmes, R. A.; Volkert, W. A.; Forster, A. M.; Weisner, P. S.; Marriott, J. A.; Chaplin, A. B. *J. Nucl. Med.* **1987**, *28*, 191−202.

(2) Leveille, J.; Demonceau, G.; DeRoo, M.; Rigo, P.; Taillefer, R.; Morgan, R. A.; Kupranick, D.; Walovitch, R. C. *J. Nucl. Med.* **1989**, *30*, 1902−1910.

(3) Moretti, J. L.; Caglar, M.; Weinmann, P. *J. Nucl. Med.* **1995**, *36*, 359−363.

(4) Papazyan, J. P.; Delavelle, J.; Burkhard, P.; Rossier, P.; Morel, P.; Maton, B.; Otten, P.; Pizzolato, G. P.; Rüfenacht, D. A.; Slosman, D. O. *J. Nucl. Med.* **1997**, *38*, 592−596.

(5) Spyriounis, D. M.; Pelecanou, M.; Stassinopoulou, C. I.; Raptopoulou, C. P.; Terzis, A.; Chiotellis, E. *Inorg. Chem.* **1995**, *34* (4), 1077−1082.

(6) Pirmettis, I. C.; Papadopoulos, M. S.; Mastrostamatis, S.; Raptopoulou, C. P.; Terzis, A.; Chiotellis, E. *Inorg. Chem.* **1996**, *35*, 1685−1691.

(7) Papadopoulos, M. S.; Pirmettis, I. C.; Pelecanou, M.; Raptopoulou, C. P.; Terzis, A.; Stassinopoulou, C. I.; Chiotellis, E. *Inorg. Chem.* **1996**, *35*, 7377−7383.

(8) Pietzsch, H. J.; Spies, H.; Hoffmann, S. *Inorg. Chim. Acta* **1989**, *165*, 163−166.

(9) Pirmettis, I. C.; Papadopoulos, M. S.; Chiotellis, E. *J. Med. Chem.* **1997**, *40*, 2539−2546.

10.1021/ic000350m CCC: $19.00
Published on Web 09/01/2000

type of monothiolate coligand are directly involved in brain uptake and retention.[9] In a further study, it was demonstrated that brain retention exhibited by many members of the ^{99m}TcO(SNS/S) series is mediated by the nucleophilic substitution of the monothiolate coligand by intracerebral glutathione (GSH) with concomitant formation of the respective daughter ^{99m}TcO(SNS/SG) hydrophilic compound.[10] The rate of this conversion is governed by electronic and steric factors imposed mainly by the N-substituent of the SNS ligand and, to a lesser extent, by the type of monothiolate coligand. Moreover, the conversion rate measured in vitro could be very well correlated to in vivo findings and especially to brain retention.[10] The product of in vitro interaction of one ReO(SNS/SG) compound with GSH has been characterized.[11]

To further investigate the influence of the N-substituent on the conversion rate of the parent MO(SNS/S) to the daughter MO(SNS/SG) complexes (M = Tc, Re), we report herein the interaction of four related oxorhenium complexes with GSH, given that rhenium is often used as a surrogate for technetium. Thus, the following ReO(L^n/L) complexes (L = C_6H_5S) were synthesized: $L^1 = C_2H_5N(CH_2CH_2S)_2$ (**1**), $L^2 = (C_2H_5)_2NCH_2CH_2N(CH_2CH_2S)_2$ (**2**), $L^3 = C_2H_5SCH_2CH_2N(CH_2CH_2S)_2$ (**3**), and L^4 = 2,6-$(HSCH_2)_2NC_5H_3$ (**4**). They were characterized by analytical methods. X-ray structure determination was performed for **3** and **4**. The interaction of complexes **1**−**4** with GSH and the formation of daughter compounds **5**−**8** were investigated by reverse-phase high-performance liquid chromatography (RP-HPLC). The kinetic aspects of this interaction were studied for complexes **1**−**3** using isothermal titration microcalorimetry. Complexes ReO(L^n/SG) (**5**−**8**) were alternatively prepared by the reaction of H_2L^n and GSH on a suitable Re(V)O precursor and were characterized by classical analytical methods. A detailed NMR study of complexes **5**−**8** was performed.

Experimental Section

Materials. All chemicals were reagent grade and used without further purification. The synthesis and purification of tridentate aminedithiol ligands, H_2L^1 ($C_2H_5N(CH_2CH_2SH)_2$), H_2L^2 ($(C_2H_5)_2NCH_2CH_2N(CH_2CH_2SH)_2$), H_2L^3 ($C_2H_5SCH_2CH_2N(CH_2CH_2SH)_2$), and H_2L^4 (2,6-$(HSCH_2)_2NC_5H_3$), were performed according to reported protocols.[12−15] Glutathione (GSH) and benzenethiol (HL) were purchased from Fluka. Rhenium was purchased from Aldrich as $KReO_4$ and was converted to the $ReOCl_3[P(C_6H_5)_3]_2$ or the $[(n\text{-}C_4H_9)_4N][ReOCl_4]$ precursor as reported previously.[16,17] Solvents for high-performance liquid chromatography (HPLC) were HPLC grade; they were passed through membrane filters (0.22 μm, Millipore) and degassed by helium flux before use. Silica gel packing material from Merck was employed for column chromatography. Thin-layer chromatography (TLC) was performed on 0.25 mm silica-gel-coated aluminium F_{254} plates from Merck. For purifications, the OASIS HLB solid-phase extraction cartridges (20 mL/1 g) from Waters were used.

Instrumentation. IR spectra were recorded on KBr pellets on a Perkin-Elmer 1600FT-IR spectrophotometer in the 500−4000 cm^{-1} region with polystyrene as a reference. ^{1}H (250.13 MHz) and ^{13}C (62.90 MHz) NMR spectra were recorded in $CDCl_3$ and D_2O (Aldrich) on a Bruker AC 250E spectrometer equipped with an Aspect 3000 Computer. Chemical shifts (δ, ppm) were referenced to TMS for samples run in $CDCl_3$ and to DSS for samples run in D_2O. Parameters for the 2D experiments (COSY, HETCOR, NOESY, etc.) have been previously reported.[5,7,18,19] Elemental analyses for C, H, N, and S were conducted on a Perkin-Elmer 2400/II Automatic Elemental Analyzer. HPLC analyses were performed on a Waters Chromatograph efficient with a 600 solvent delivery system and coupled to a Waters 996 Photodiode Array UV Detector. The Millennium Software from Waters was applied for controlling the HPLC system and processing the data. The conditions for the analyses are given for individual products below. For product purification, a preparative HPLC system from Waters was used (Waters Prep LC 4000) coupled to the PDA UV detector used also for analyses. For separations, a Prep Nova-Pak HR C18 cartridge (25 mm × 100 mm, 6 μm) from Waters was used. Microcalorimetric studies have been carried out on an isothermal titration calorimeter (MCS-ITC, Microcal). Thermal data have been analyzed using the Origin 5.0 software.

Synthesis of ReO(L^n/L) Complexes. ReO{$[C_2H_5N(CH_2CH_2S)_2][SC_6H_5]$} (1). Synthesis and analytical data for **1** have been reported elsewhere.[6]

ReO{$[(C_2H_5)_2NCH_2CH_2N(CH_2CH_2S)_2][SC_6H_5]$} (2). This compound has been synthesized and characterized as previously reported.[6,7]

ReO{$[C_2H_5SCH_2CH_2N(CH_2CH_2S)_2][SC_6H_5]$} (3). To a suspension of $ReOCl_3[P(C_6H_5)_3]_2$ (166.6 mg, 0.2 mmol) and CH_3COONa (164 mg, 2 mmol) in MeOH (25 mL), a solution of $C_2H_5SCH_2CH_2N(CH_2CH_2SH)_2$ (45.0 mg, 0.2 mmol) and C_6H_5SH (22.0 mg, 0.2 mmol) in MeOH (5 mL) was added under stirring. The mixture was refluxed under stirring until a clear solution formed while its color changed from yellow-green to dark-green. After the addition of CH_2Cl_2 (15 mL) and H_2O (10 mL), two layers separated. The organic layer was collected, dried over $MgSO_4$, and filtered through a paper filter. The clear bright green filtrate was concentrated to a small volume under vacuum, and a small amount of MeOH was added. By slow evaporation at ambient temperature, green needlelike crystals of complex **3** separated. Yield: 65%. R_f (SiO_2; CH_2Cl_2): 0.5. t_R (HPLC Techsil RP C18, 10 μm, 4.6 mm × 250 mm, 80:20 MeOH/H_2O, isocratic): 4.54 min. Anal. Calcd for $C_{14}H_{22}NOReS_4$: C, 31.44; H, 4.15; N, 2.62; S, 23.98. Found: C, 31.52; H, 3.99; N, 2.73; S, 24.02. UV−vis (80:20 MeOH/H_2O, λ/nm): 412. IR (KBr, cm^{-1}): 3441, 2961, 2927, 1453, 1437, 1270, 944 (Re═O str.). ^{1}H NMR (CD_3Cl): δ 3.52 and 2.87 (4H, m, br, SCH_2CH_2NReO), 3.32 and 2.73 (4H, m, br, SCH_2CH_2NReO), 4.00 (2H, m, NCH_2CH_2SEt), 2.96 (2H, m, NCH_2CH_2SEt), 2.63 (2H, q, SCH_2CH_3), 1.30 (3H, t, SCH_2CH_3), 7.65 (2H, m, *o*-Ar−H), 7.40 (2H, m, *m*-Ar−H), 7.21 (1H, m, *p*-Ar−H). ^{13}C NMR (CD_3Cl): δ 41.93 (SCH_2CH_2NReO), 63.10 (SCH_2CH_2NReO), 63.63 (NCH_2CH_2SEt), 25.57 (NCH_2CH_2SEt), 26.58 (SCH_2CH_3), 14.65 (SCH_2CH_3), 153.64 (*i*-Ar), 133.52 (*o*-Ar), 127.97 (*m*-Ar), 126.57 (*p*-Ar).

ReO{$[2,6\text{-}(CH_2S)_2NC_5H_3][SC_6H_5]$} (4). To a suspension of $[(n\text{-}C_4H_9)_4N][ReOCl_4]$ (146.6 mg, 0.25 mmol) in EtOH (2 mL) cooled to 0 °C, a solution of 2,6-$(HSCH_2)_2NC_5H_3$ (43 mg, 0.25 mmol) and C_6H_5SH (28 μL, 0.275 mmol) in $CHCl_3$ (1 mL) was added under stirring. This mixture was stirred at 0 °C for 2 h and then stirred overnight at ambient temperature while its color changed to red. The solvent was expelled under vacuum, and the red residue was redissolved in a small portion of $CHCl_3$. The red solution was loaded on a silica gel column (3 cm × 10 cm), which was eluted with $CHCl_3$. The fraction containing the red product was collected and concentrated to a small volume under vacuum, and a small amount of MeOH was added. Slow evaporation of the dark red solution at ambient temperature afforded red needlelike crystals of complex **4**. Yield: 51%. R_f (SiO_2; $CHCl_3$): 0.3. Mp: 231−233 °C. t_R (HPLC Techsil RP C18, 10 μm, 4.6 mm × 250 mm, 60:40 MeOH/H_2O, isocratic): 12.8 min. Anal. Calcd for $C_{13}H_{12}NOReS_3$: C, 32.49; H, 2.52; N, 2.91; S, 20.01. Found: C, 31.91; H, 2.63; N, 2.94;

(10) Nock, B. A.; Maina, T.; Yannoukakos, D.; Pirmettis, I. C.; Papadopoulos, M. S.; Chiotellis, E. *J. Med. Chem.* **1999**, *42*, 1066−1075.
(11) Pelecanou, M.; Pirmettis, I. C.; Nock, B. A.; Papadopoulos, M.; Chiotellis, E.; Stassinopoulou, C. I. *Inorg. Chim. Acta* **1998**, *281*, 148−152.
(12) Corbin, J.-L.; Miller, K. F.; Pariyadath, N.; Wherland, S.; Bruce, L. A.; Stiefel, E. I. *Inorg. Chim. Acta* **1984**, *90*, 41−51.
(13) Mann, F. *J. Chem. Soc.* **1934**, 461−466.
(14) Harley-Mason, J. *J. Chem. Soc.* **1947**, 320−322.
(15) Nock, B.; Pietzsch, H.-J.; Tisato, F.; Maina, T.; Leibnitz, P.; Spies, H.; Chiotellis, E. *Inorg. Chim. Acta* **2000**, *304*, 26−32.
(16) Rouschias, G. *Chem. Rev.* **1974**, *74*, 531−566.
(17) Alberto, R.; Schibli, R.; Egli, A.; Schubiger, P. A.; Herrmann, W. A.; Artus, G.; Abram, U.; Kaden, T. A. *J. Organomet. Chem.* **1995**, *492*, 217−224.
(18) Stassinopoulou, C. I.; Pelecanou, M.; Mastrostamatis, S.; Chiotellis, E. *Magn. Reson. Chem.* **1994**, *32*, 532−536.
(19) Papadopoulos, M. S.; Pelecanou, M.; Pirmettis, I. C.; Spyriounis, D. M.; Raptopoulou, C. P.; Terzis, A.; Stassinopoulou, C. I.; Chiotellis, E. *Inorg. Chem.* **1996**, *35*, 4478−4483.

S, 19.68. UV−vis (60:40 MeOH/H_2O, λ/nm): 286, 364. IR (KBr, cm^{-1}): 3431, 2963, 2873, 1621, 1584, 1455, 1443, 1310, 1270, 1122, 1097, 998, 968 (Re═O str.), 905, 856. ^1H NMR ($CDCl_3$): δ 5.37 and 4.97 [4H, br, 2,6-(SCH_2)$_2$N], 7.78 (2H, br, 3,5-pyr), 7.95 (1H, m, 4-pyr), 7.70 (2H, m, *o*-Ar), 7.41 (2H, m, *m*-Ar), 7.24 (1H, m, *p*-Ar). ^{13}C NMR ($CDCl_3$): δ 53.26 [2,6-(SCH_2)$_2$N], 173.48 (2,6-pyr), 118.94 (3,5-pyr), 140.67 (4-pyr), 149.01 (*i*-Ar), 133.94 (*o*-Ar), 128.01 (*m*-Ar), 127.10 (*p*-Ar).

Synthesis of ReO(L^n/SG) Complexes. Method A: From the ReOCl$_3$[P(C$_6$H$_5$)$_3$]$_2$ Precursor. ReO{[C$_2$H$_5$N(CH$_2$CH$_2$S)$_2$][SG]} (5). To an aqueous solution of CH_3COONa (164 mg, 2 mmol in 1 mL of H_2O), a solution of GSH (615 mg, 2 mmol) in H_2O (5 mL) was added under stirring, followed by a solution of the $C_2H_5N(CH_2CH_2SH)_2$ ligand (33 mg, 0.2 mmol) in MeOH (5 mL). The $ReOCl_3[P(C_6H_5)_3]_2$ precursor (166.6 mg, 0.2 mmol) was then added, and the pH of the mixture was adjusted to 7 by adding a small amount of 1 N NaOH. The mixture was refluxed under stirring until a clear solution was obtained. This was concentrated to a small volume and then loaded on an activated OASIS solid-phase extraction cartridge; the cartridge was rinsed with H_2O, and the complex was eventually collected in MeOH. This solution was concentrated to a small volume under a nitrogen stream and then purified by preparative HPLC. The column was eluted at 10 mL/min with 75:25 MeOH/0.2% triethylammonium phosphate (TEAP) at pH 7.1. The fraction eluting at 7 min was collected and loaded again on an activated OASIS cartridge. The cartridge was rinsed first with physiological saline and then with H_2O, and the complex was collected in MeOH. For analyses, the solvent was evaporated under vacuum, and the oily residue was redissolved in a small quantity of H_2O. The solution was lyophilized to afford a green powder. Yield: 35%. t_R (HPLC RP C18 Merck Lichrospher 100, 10 μm, 4.6 mm × 250 mm, MeOH for method A or 2% Et_3N/H_3PO_4 for method B, pH 7.1, 100% MeOH to 10% MeOH from 1 to 35 min): 13.7 min. Anal. Calcd for $C_{16}H_{29}N_4O_7ReS_3$: C, 28.61; H, 4.35; N, 8.34; S, 14.32. Found: C, 29.01; H, 4.63; N, 8.22; S, 14.65. ES$^-$-MS: 671.02 (calcd, 671.82). UV−vis (MeOH or 2% Et_3N/H_3PO_4, pH 7.1, λ/nm): 264, 378, 580. IR (KBr, cm^{-1}): 3376, 2927, 1652, 1558, 1539, 1399, 1268, 948 (Re═O str.). Relevant ^1H and ^{13}C NMR data are summarized in Tables 3 and 4.

ReO{[(C$_2$H$_5$)$_2$NCH$_2$CH$_2$N(CH$_2$CH$_2$S)$_2$][SG]} (6). The preparation of complex **6** has been described previously, and relevant analytical data have been published.[10,11] Some additional data are given below. t_R (HPLC RP C18 Waters Symmetry Shield, 5 μm, 3.9 mm × 150 mm, MeOH for method A or 2% Et_3N/H_3PO_4 for method B, pH 7.0, 10% MeOH to 50% MeOH from 1 to 20 min): 9.46 min;. Anal. Calcd for $C_{20}H_{38}N_5O_7ReS_3$: C, 32.29; H, 5.15; N, 9.42; S, 12.91. Found: C, 31.92; H, 4.98; N, 9.57; S, 13.03. UV−vis (MeOH or 2% Et_3N/H_3PO_4, pH 7.0, λ/nm): 265, 386, 591. IR (KBr, cm^{-1}): 3278, 2925, 1652, 1539, 1395, 1267, 947 (Re═O str.).

ReO{[C$_2$H$_5$SCH$_2$CH$_2$N(CH$_2$CH$_2$S)$_2$][SG]} (7). To a suspension of $ReOCl_3[P(C_6H_5)_3]_2$ (166.6 mg, 0.2 mmol) in a 1:1 DMF/H_2O mixture (20 mL), the $C_2H_5SCH_2CH_2N(CH_2CH_2SH)_2$ ligand (44 mg, 0.2 mmol) and a solution of GSH (615 mg, 2 mmol) in H_2O (10 mL) were added under stirring. The color of the reaction mixture changed from bright yellow to orange upon the addition of GSH. When the pH was adjusted to 7 by the addition of 1 N NaOH, the color of the solution changed to green. The mixture was refluxed under stirring for 1 h while its color turned dark cypress green. When the mixture reached ambient temperature, H_2O (10 mL) was added, and the mixture was washed with CH_2Cl_2 (3 × 10 mL). The aqueous phase was loaded on an activated OASIS solid-phase extraction cartridge. The cartridge was rinsed with H_2O, and the complex was collected in MeOH. For analyses, MeOH was expelled under vacuum, and the oily residue was redissolved in a small portion of H_2O. The aqueous solution was eventually lyophilized to afford a green powder. Yield: 40%. t_R (HPLC RP C18 Merck Lichrospher 100, 10 μm, 4.6 mm × 250 mm, MeOH for method A or 2% Et_3N/H_3PO_4 for method B, pH 7.1, 100% MeOH to 10% MeOH from 1 to 20 min): 16.3 min. Anal. Calcd for $C_{18}H_{33}N_4O_7ReS_4$: C, 29.54; H, 4.54; N, 7.65; S, 17.52. Found: C, 30.02; H, 4.48; N, 7.72; S, 17.43. ES$^-$-MS: 730.93 (calcd, 730.93). UV−vis (MeOH or 2% Et_3N/H_3PO_4, pH 7.1, λ/nm): 265, 385, 591. IR (KBr, cm^{-1}): 3278, 2925, 1652, 1539, 1395, 1267, 947 (Re═O str.). Relevant ^1H and ^{13}C NMR data are summarized in Tables 3 and 4.

ReO{[2,6-(SCH$_2$)$_2$NC$_5$H$_3$][SG]} (8). The $ReOCl_3[P(C_6H_5)_3]_2$ precursor (166.6 mg, 0.2 mmol) was suspended in a 1:2 DMF/H_2O mixture (30 mL), and the 2,6-$(HSCH_2)_2NC_5H_3$ ligand (34.2 mg, 0.2 mmol) and a solution of GSH (615 mg, 2 mmol) in H_2O (10 mL) were added under stirring. The pH was adjusted to 7 by the addition of 1 N NaOH (2.5 mL), and DMF was subsequently added (20 mL). The orange mixture was refluxed under stirring for 60 min and purified first on an OASIS solid extraction cartridge and then by preparative HPLC, as described for complex **5**. The product collected at 10 min was desalted with an OASIS cartridge and finally collected pure in MeOH. For analyses, the solvent was evaporated to dryness, and the oily residue was redissolved in a small volume of H_2O. The solution was lyophilized to afford an orange powder. Yield: 30%. t_R (HPLC RP C18 Merck Lichrospher 100, 10 μm, 4.6 mm × 250 mm, MeOH for method A or 2% Et_3N/H_3PO_4 for method B, pH 7.1, 100% MeOH to 10% MeOH from 1 to 20 min): 15.03 min. Anal. Calcd for $C_{17}H_{25}N_4O_7ReS_3$: C, 30.04; H, 3.71; N, 8.24; S, 14.15. Found: C, 30.12; H, 4.06; N, 7.96; S, 14.30. ES$^-$-MS: 676.93 (calcd, 676.78). UV−vis (MeOH or 2% Et_3N/H_3PO_4, pH 7.1, λ/nm): 279, 348. IR (KBr, cm^{-1}): 3398, 1646, 1602, 1463, 1397, 1298, 1022, 966 (Re═O str.). Relevant ^1H and ^{13}C NMR data are summarized in Tables 3 and 4.

Method B: From the Parent ReO(L^n/L) Complexes after Reaction with GSH. The parent ReO(L^n/L) complex was dissolved to 1 mM concentration in CH_2Cl_2, and an aliquot (1 mL) was placed in a penicillin vial. This solution was reduced to a small volume (~20 μL) under a gentle stream of nitrogen at 25 °C and then diluted with EtOH (1 mL). To this, a 0.2 M GSH solution (500 μL) was added, followed by the addition of a 0.2 M phosphate buffer at pH 7.4 (500 μL). The pH of this mixture was adjusted to 7.4 with 1 N NaOH, and the vial was sealed under nitrogen and incubated at 37 °C. Formation of the respective daughter complexes ReO(L^n/GS) was followed by HPLC, as described above.

X-ray Crystal Structure Determination of ReO(L^n/L) Complexes. Diffraction measurements for **3** and **4** were performed on a Crystal Logic Dual Goniometer diffractometer using graphite-monochromated Mo radiation. Unit cell dimensions were determined and refined by using the angular settings of 25 automatically centered reflections in the range of $11° < 2\theta < 23°$, and they appear in Table 1. Intensity data were recorded using the $\theta-2\theta$ scan. Three standard reflections monitored every 97 reflections showed less than 3% variation and no decay. Lorentz, polarization, and ψ-scan absorption corrections (only for **3**) were applied using the Crystal Logic software. The structures were solved by direct methods using SHELXS-86[20] and refined by full-matrix least-squares techniques on F^2 with SHELXL-93.[21,22] Compound **3** crystallizes in the triclinic space group $P\bar{1}$, while **4** crystallizes in the monoclinic space group $P2_1/a$ with two molecules per asymmetric unit. All non-hydrogen atoms for both structures were refined anisotropically. All hydrogen atoms in **3** (except those of the methyl group, which were introduced at calculated positions as riding on bonded atoms) were located by difference maps and refined isotropically. All hydrogen atoms in **4** were introduced at calculated positions as riding on bonded atoms.

Thermodynamic Study of the Interaction of ReO(L^n/L) Complexes with GSH. Kinetic Aspects of the Interaction. Isothermal titration microcalorimetry was employed to provide a comparative kinetic study of the reaction of the ReO(L^n/L) complexes with GSH in aqueous DMF. Single-injection titration experiments were carried out to monitor the rate of heat release or absorption as a function of time and to calculate reaction rates. For the microcalorimetric measurements, a fresh 5×10^{-5} M solution of the respective ReO(L^n/L) in aqueous DMF was prepared as follows: the complex was dissolved in DMF to a 1 mM concentration; to an aliquot of this solution (50 μL), a mixture

(20) Sheldrick, G. M. *SHELXS-86: Structure Solving Program*; University of Göttingen: Göttingen, Germany, 1986.
(21) Sheldrick, G. M. *SHELXL-93: Crystal Structure Refinement*; University of Göttingen: Göttingen, Germany, 1993.
(22) Addison, A. W.; Rao, T. N.; Reedijk, J.; Rijn, J.; Verschoor, G. C. *J. Chem. Soc., Dalton Trans.* **1984**, 1349−1356.

Scheme 1. Synthesis of ReO(L^n/L) Complexes

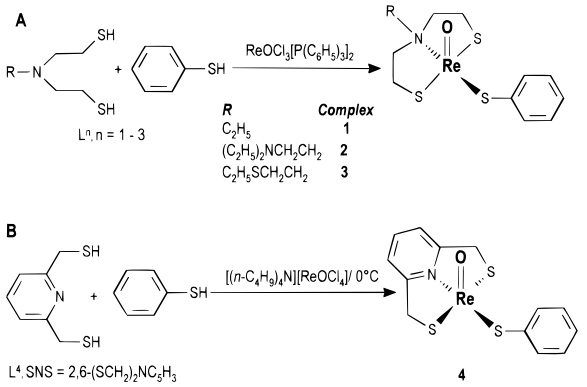

of DMF (450 μL), H_2O (450 μL), and 0.2 M phosphate buffer at pH 7.4 (50 μL) was added to an end volume of 1 mL. A fresh 1 mM solution of GSH in aqueous DMF was prepared as follows: an aliquot (300 μL) of a 10 mM GSH solution was mixed with H_2O (1050 μL), DMF (1.5 mL), and 0.2 M phosphate buffer at pH 7.4 (50 μL) to an end volume of 3 mL.

All the samples were degassed in a vacuum for a period of 15 min prior to loading to the microcalorimeter. An aliquot (1.3 mL) of the 1 mM GSH solution (titrand) was loaded into the titration cell of the microcalorimeter, and exactly the same volume of distilled water was loaded to the reference cell. Both cells were placed in an adiabatic jacket. A 250 μL titration syringe was filled with the 5×10^{-5} M solution of the respective ReO(L^n/L) complex (titrant). The injection syringe was precision bore glass with a stir paddle attached to the extreme end. The syringe plunger was mechanically coupled to a precision digital stepping motor (6400 steps/in.). For all the single-injection experiments, a 10 μL injection was scheduled at 37 °C and a 400 rpm stirring rate after an initial delay of 400 s. The injection lasted for 6.3 s and produced complete mixing. The rate of heat release or heat absorption was expressed as the electric power needed to maintain the temperature difference between sample and reference cells at zero. This rate was automatically recorded by a Pentium II PC.

For each titration experiment, the contributions to heat release or absorption rates from the dilution of the 5×10^{-5} M solution of the respective ReO(L^n/L) complex to 1.33 mL of aqueous DMF and from the dilution of the 1 mM GSH solution by the titration of 10 μL of aqueous DMF were measured in separate experiments identical to the original one. These contributions were then subtracted from the raw titration data. To check for possible contributions to the heat rates by differences in the water/DMF ratio of the solvents that may arise from the degassing process, we performed several experiments for various degassing periods, and these contributions were found to be negligible.

Results and Discussion

Synthesis. The ReO(L^n/L) complexes **1**−**3** were prepared from the $ReOCl_3[P(C_6H_5)_3]_2$ precursor by a slight modification of reported methods,[6,7] whereas complex **4** was synthesized by reacting equimolar quantities of the 2,6-$C_6H_3N(CH_2SH)_2$ and C_6H_5SH ligands with the $[(n\text{-}C_4H_9)_4][ReOCl_4]$ precursor in a chilled $EtOH/CH_2Cl_2$ mixture.[15] Syntheses were completed in good yields and are depicted in Scheme 1. Daughter complexes **5**−**8** were obtained through two synthetic routes, shown in Scheme 2. Briefly, the respective tridentate SNS ligand and GSH were reacted via method A with the $ReOCl_3[P(C_6H_5)_3]_2$ precursor in a 1:10:1 molar ratio in refluxing aqueous DMF or aqueous MeOH mixtures. Complexes **5**−**8** were obtained in relatively good yields after purification through a battery of solid-phase extraction cartridges and semipreparative RP-HPLC. From the alternative method B, the reaction of a high molar excess of GSH with parent complexes **1**−**4** in an (pH 7.4) EtOH buffer mixture at 37 °C leads quantitatively to the respective daughter complexes **5**−**8**, wherein the C_6H_5S coligand has been replaced

Scheme 2. Syntheses of ReO(L^n/SG) Complexes (A) from the $ReOCl_3[P(C_6H_5)_3]_2$ Precursor (method A) and (B) from Parent ReO(L^n/L) Complexes by Action of GSH (method B)

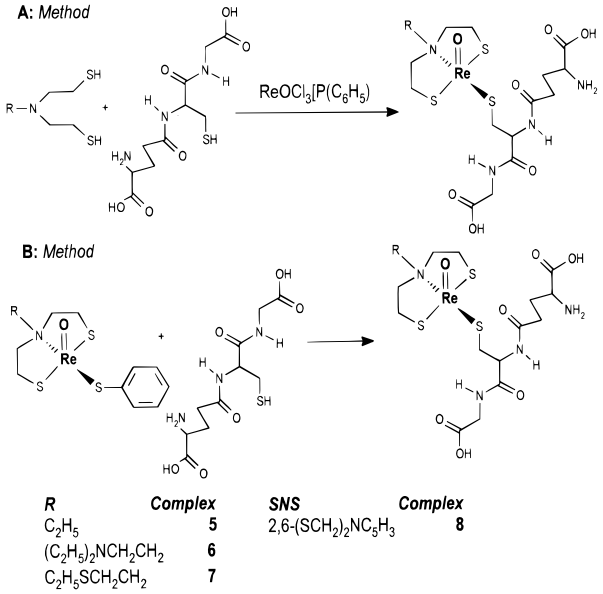

by GS. Kinetic aspects for this reaction will be discussed in detail in a special section below.

Characterization. Analytical data, given in the Experimental Section, confirm the formulas assigned to the ReO(L^n/L) complexes **3** and **4**. Elemental analyses as well as TLC and HPLC chromatographs confirm the purity of the complexes. The UV profiles of the compounds show maxima at 412 and 364 nm, which fall within the range of values reported for similar complexes.[7] The IR spectra show bands at 944 and 968 cm^{-1}, assigned to the Re═O stretching vibration and in agreement with reported values for similar oxorhenium compounds.[7] Additional X-ray diffraction analysis for **3** and **4** and relevant ^1H and ^{13}C NMR data support the formation of the compounds (see Table 1).

The formation of daughter complexes ReO(L^n/SG), **5**−**8**, either through method A or through method B, was verified by elemental analysis and ES-MS. Analytical RP-HPLC confirmed the purity of the compounds. UV spectra showed maxima at 385 (for **5**−**7**) or 348 nm (for **8**), assigned to ReO−S charge-transfer bands, as reported for similar compounds.[7,11] The Re═O stretching vibration is evidenced by a band at 947 cm^{-1} in the IR spectra of **5**−**7** and at 966 cm^{-1} in the spectrum of **8**, thus in the same range of values as their respective parent ReO(L^n/L) complexes. Structure analysis of compounds **5**−**8** was mainly based on NMR studies and will be discussed exhaustively in a special section below.

Description of the Structures. An ORTEP diagram of **3** is shown in Figure 1, and selected bond distances and angles are listed in Table 2. The coordination geometry about rhenium is distorted trigonal bipyramidal, with the sulfur atoms of the tridentate ligand and the oxo group in the basal plane, while the nitrogen of the latter ligand and the monodentate thiol are directed in the apical positions. The angles in the basal plane are close to the ideal value of 120° (117.6(1)−123.31(4)°), but the distortion of the trigonal bipyramid comes via the deviation from 180° of the S(3)−Re−N(1) angle (159.49(9)°). Thus, the calculated trigonality index, τ,[23] is 0.60, a value which has also

(23) Rabenstein, D. L.; Millis, K. K. *Biochim. Biophys. Acta* **1995**, *1249*, 29−36.

Table 1. Summary of Crystal Data for Compounds **3** and **4**

	3	**4**
empirical formula	$C_{14}H_{22}NOReS_4$	$C_{13}H_{12}NOReS_3$
formula weight	534.77	480.64
temp	298 K	298 K
wavelength	0.71073 Å	0.71073 Å
space group	*P*1	$P2_1/a$
a	11.086(8) Å	12.50(2) Å
b	8.624(6) Å	22.63(4) Å
c	10.906(7) Å	10.49(2) Å
α	93.06(2)°	−
β	110.53(2)°	101.37(4)°
γ	75.06(2)°	−
V, *Z*	943(1) Å^3, 2	2910(8) Å^3, 8
D_{calcd}	1.884 Mg/m^3	2.194 Mg/m^3
abs coeff	6.886 mm^{-1}	8.771 mm^{-1}
cryst size	0.15 × 0.30 × 0.50 mm^3	0.10 × 0.20 × 0.50 mm^3
reflns collected	3493	4410
independent reflns	3306 [R_{int} = 0.0067]	4158 [R_{int} = 0.0886]
data/restraints/parameters	3306/0/268	4065/0/351
goodness-of-fit on F^2	1.135	1.044
observed reflns [$I > 2\sigma(I)$]	3241	3161
final R indices [$I > 2\sigma(I)$]	R1 = 0.0181, wR2 = 0.0517	R1 = 0.0633, wR2 = 0.1421
R indices (all data)	R1 = 0.0186, wR2 = 0.0522	R1 = 0.0889, wR2 = 0.1648

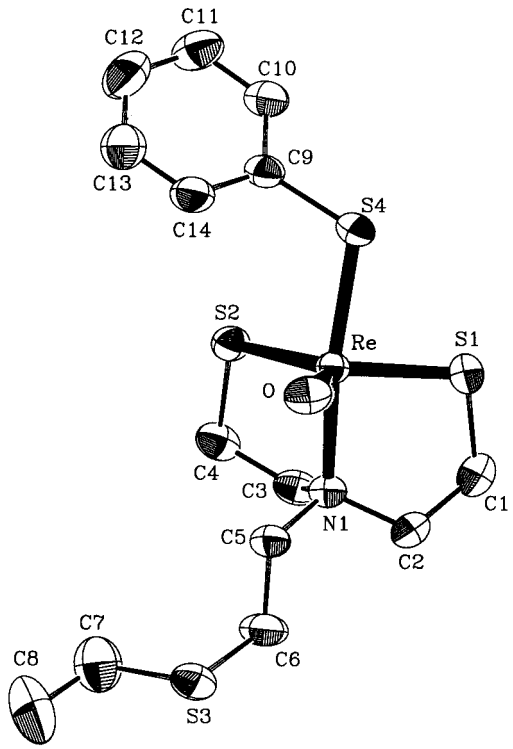

Figure 1. ORTEP diagram of complex **3**.

been found in analogous complexes.[7] The complex is the syn isomer with the N-substituent cis to the oxo group (C(5)···O = 2.946(1) Å). The two five-membered rings in the coordination sphere adopt the stable envelope configuration with the carbon atoms adjacent to N(1) being out of the mean plane of the remaining four atoms (displacements of 0.57 and 0.64 Å for C(2) and C(3), respectively). The torsion angles of the tridentate chelating backbone are 46.5(6)° and 51.7(5)° for S1−C1−C2−N1 and N1−C3−C4−S2, respectively.

An ORTEP diagram of one of the crystallographically independent molecules of **4** is given in Figure 2, and bond distances and angles of the coordination sphere are listed in Table 2. Inspection of the shape-determining angles around rhenium gives values of 0.14 (mol1) and 0.20 (mol2) for τ; thus, the coordination geometry is described as square pyramidal

Table 2. Selected Bond Distances (Å) and Angles (deg)

		4	
	3	mol1	mol2
Re−O	1.695(3)	1.70(1)	1.67(1)
Re−N(1)	2.214(3)	2.11(2)	2.13(2)
Re−S(1)	2.276(2)	2.272(6)	2.281(6)
Re−S(2)	2.279(2)	2.279(6)	2.289(6)
Re−S(3)	2.307(2)	2.294(7)	2.302(6)
O−Re−N(1)	95.7(1)	108.1(6)	105.9(6)
O−Re−S(1)	117.6(1)	111.8(5)	112.1(4)
N(1)−Re−S(1)	83.95(9)	81.2(4)	80.5(4)
O−Re−S(2)	118.5(1)	111.0(5)	111.6(4)
N(1)−Re−S(2)	83.39(9)	80.8(4)	80.3(4)
S(1)−Re−S(2)	123.31(4)	136.8(2)	135.6(2)
O−Re−S(3)	104.61(9)	106.3(6)	106.1(4)
N(1)−Re−S(3)	159.49(9)	145.2(4)	147.5(4)
S(1)−Re−S(3)	84.37(5)	90.8(2)	92.0(2)
S(2)−Re−S(3)	89.03(6)	82.5(2)	83.5(2)

(τ = 0 for perfect sp and τ = 1 for perfect tbp), with the S−Re−S and S−Re−N angles severely deviating from the ideal 180° (136.8(2)° and 145.2(4)° for mol1 and 135.6(2)° and 147.5(4)° for mol2). Rhenium lies ∼0.73 Å out of the basal plane of the distorted square pyramid toward the oxo group in both mol1 and mol2. The two five-membered rings in the coordination sphere (defined by Re1, S1, C1, C2, and N1 and Re1, S2, C7,C6, and N1) exist in the envelope configuration with Re(1) and S(2) 0.59 and 0.75 Å out of the mean plane of the remaining four atoms in mol1, respectively, while the metal is the "flap" atom in the corresponding five-membered rings in mol2 (displacements of 0.72 and 0.80 Å). The torsion angles of the tridentate chelating backbone, i.e., the S1−C1−C2−N1 and N1−C6−C7−S2, are −4.9(1)° and 17.0(1)° in mol1, and the corresponding angles in mol2 are 10.5(1)° and −12.7(1)° for S11−C21−C22−N11 and N11−C26−C27−S12, respectively. The bond distances in the coordination sphere of both **3** and **4** are in the ranges observed in analogous complexes.[7,15]

Structural Study of Complexes 5, 7, and 8 with NMR. The NMR spectra of compounds **5** (pH 6.9), **7** (pH 6.6), and **8** (pH 6.9) were recorded in D_2O at 298 K. The pH of the samples is reported uncorrected for isotope effects. ^{1}H and ^{13}C chemical shifts are summarized in Tables 3 and 4. The numbering of the complexes is shown in Scheme 3 (lettering of the GS moiety is made according to the literature[23,24] to facilitate comparisons).

Table 3: ^{1}H Chemical Shifts, δ_H, for Compounds **5**, **7**, and **8** in D_2O at 298 K

	5 (pH 6.9)	**7** (pH 6.6)		**8** (pH 6.9)
H1 and H4 endo[a]	3.70[b]	3.73[b]	H1 and H2 endo[a]	5.43, 5.40
H1 and H4 exo[a]	3.01	3.07[b]	H1 and H2 exo	4.91
H2 and H3 endo[a]	3.39	3.45	H3′ and H5′	7.83 (J = 7.8 Hz)
H2 and H3 exo[a]	2.73	2.80	H4′	8.02 (J = 7.8 Hz)
H5	3.84	3.94[b]		
H6	1.35	3.10[b]		
H7		2.63		
H8		1.24		
H-g1	3.80, 3.71[c] (J = 17.2 Hz)	3.85, 3.76[c] (J = 17.4 Hz)	H-g1	3.83, 3.74 (J = 17.3 Hz)[c]
H-g2	4.12, 3.94[b]	4.12, 3.97[b]	H-g2	4.13 (J = 13.8, 4.5 Hz) 3.95 (J = 13.8, 9.3 Hz)
H-g3	2.46	2.46	H-g3	2.48
H-g4	2.08	2.09	H-g4	2.10
H-g5	4.79[b]	4.79[b]	H-g5	4.91 (J = 9.3, 4.5 Hz)
H-g6	3.70[b]	3.72	H-g6	3.71

[a] Endo protons are those oriented toward oxygen, while exo protons are those oriented away from oxygen. [b] Chemical shifts of overlapping multiplets were defined from the correlation peaks of the 2D experiments. [c] The linear midpoint (instead of the center of gravity) of the doublets is reported as a shift position.

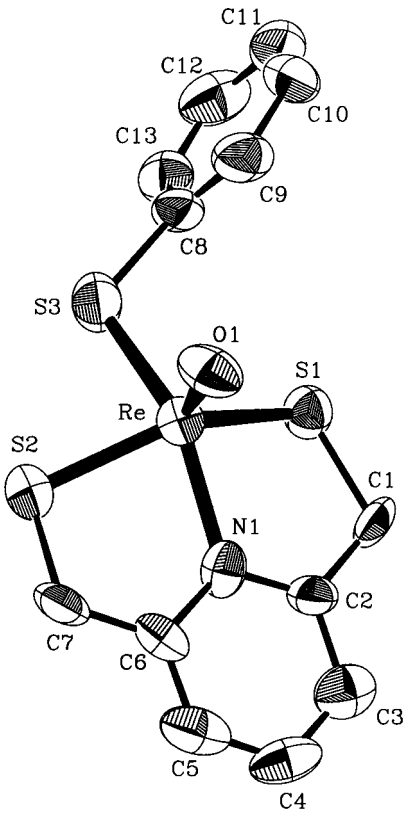

Figure 2. ORTEP diagram of complex **4**.

^{1}H and ^{13}C chemical shifts for compound **6** have been previously reported.[11]

The observed spectra of **5**, **7**, and **8** are consistent with the proposed structures wherein the tridentate aminedithiol ligand wraps around the ReO core and the glutathione molecule, acting as a monodentate ligand, occupies the fourth coordination site to give mixed-ligand ReO(L^n/SG) complexes. As evidenced by integration of the peaks, resonances corresponding to the coordinated GS and the L^n aminedithiol ligands are present in a 1:1 ratio. The ^{1}H−^{1}H correlation spectrum of complex **5** is displayed in Figure 3.

In all complexes, carbon resonances C-g1, C-g3, C-g4, C-g5, and C-g6 of the metal-bound GS are very close (±0.1−0.5 ppm) to those of free GSH (recorded for reference at pH 7.0). However, the resonance corresponding to carbon C-g2 is shifted downfield by 17.7 ppm in **5**, 18.5 ppm in **7**, and 15.0 ppm in **8**.

Table 4: ^{13}C Chemical Shifts, δ_C, for Compounds **5**, **7**, and **8** in D_2O at 298 K

	5 (pH 6.9)	**7** (pH 6.6)		**8** (pH 6.9)
C1 and C4	43.80, 43.67	44.18, 44.05	C1 and C2	54.8[a]
C2 and C3	64.40, 64.16	65.10, 64.88	C2′ and C6′	174.56
C5	62.01	66.28	C3′ and C5′	122.36
C6	10.94	27.12	C4′	144.86
C7		28.15		
C8		16.70		
C-g1	46.10	45.70	C-g1	46.18
C-g2	45.88	46.69	C-g2	43.21
C-g3	34.20	34.17	C-g3	34.20
C-g4	28.90	28.90	C-g4	28.93
C-g5	58.81	58.80	C-g5	58.69
C-g6	56.86	56.82	C-g6	56.87

[a] The center of the broad peak belonging to C-1 and C-2 is reported.

Scheme 3. Structures of Complexes **5**, **7**, and **8** Studied by NMR, Showing the Numbering of the Atoms Used in the Assignments

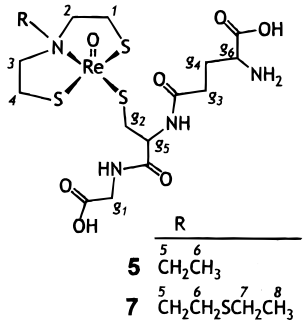

5 R = $^{5}CH_2{}^{6}CH_3$

7 R = $^{5}CH_2{}^{6}CH_2{}^{7}SCH_2{}^{8}CH_3$

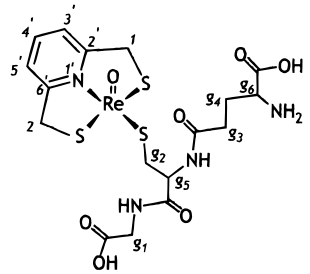

8

(24) Lempers, E. L. M.; Inagaki, K.; Reedijk, J. *Inorg. Chim. Acta* **1988**, *152*, 201−207.

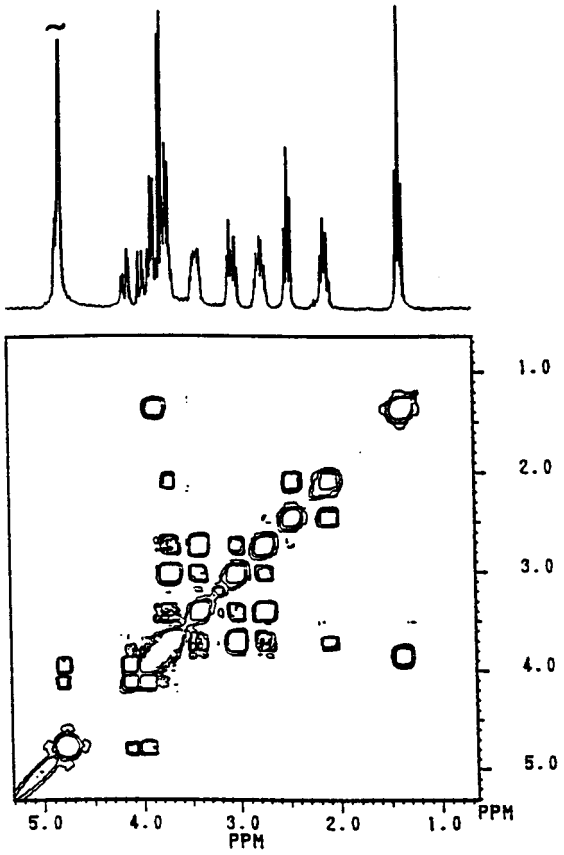

Figure 3. $^1H-^1H$ correlation spectrum (COSY) for complex **5** in D_2O at 298 K.

These findings are consistent with the GSH binding the oxorhenium core through the SH moiety of cysteine. Accordingly, the cysteine H-g2 proton resonances (at 4.12 and 3.94 ppm in **5**, 4.12 and 3.97 ppm in **7**, and 4.13 and 3.95 ppm in **8**) are shifted downfield as compared to their position in free GSH (2.92 and 2.97 ppm).

The H-g1 protons of coordinated GS in **5**, **7**, and **8** appear as two closely spaced doublets, while in free GSH, they show up as a singlet peak. Apparently, this change is caused by the increased asymmetry introduced to the GSH molecule upon coordination to the monooxorhenium core.

Chemical shifts of protons and carbons of the coordinating SNS ligand backbone of **5** and **7** are within the range of values reported previously for analogous oxorhenium SNS/S-type complexes[7,11] and in complete agreement with the proposed structures. Furthermore, it has been well documented in previous studies on the SNS/S type of oxorhenium complexes that assignment of the direction of the pendant N-substituent chain toward the ReO core (syn configuration) or away from it (anti configuration) can be based exclusively on NMR data.[7] On the basis of the appearance of the spectra as well as the observed chemical shifts of **5** and **7**, it can be safely concluded that the complexes adopt the syn configuration with the side chain on the nitrogen directed toward the ReO core.

Carbons C1 and C4 as well as C2 and C3 of complexes **5** and **7** appear as separate—but very closely spaced—peaks due to the asymmetry of the molecules. In the ^1H spectra, the differentiation of the two sides is not clear due to peak overlapping, and the H1 and H4 protons, as well as H2 and H3 protons, appear as broad multiplets (the linear midpoint of which is reported in Table 3).

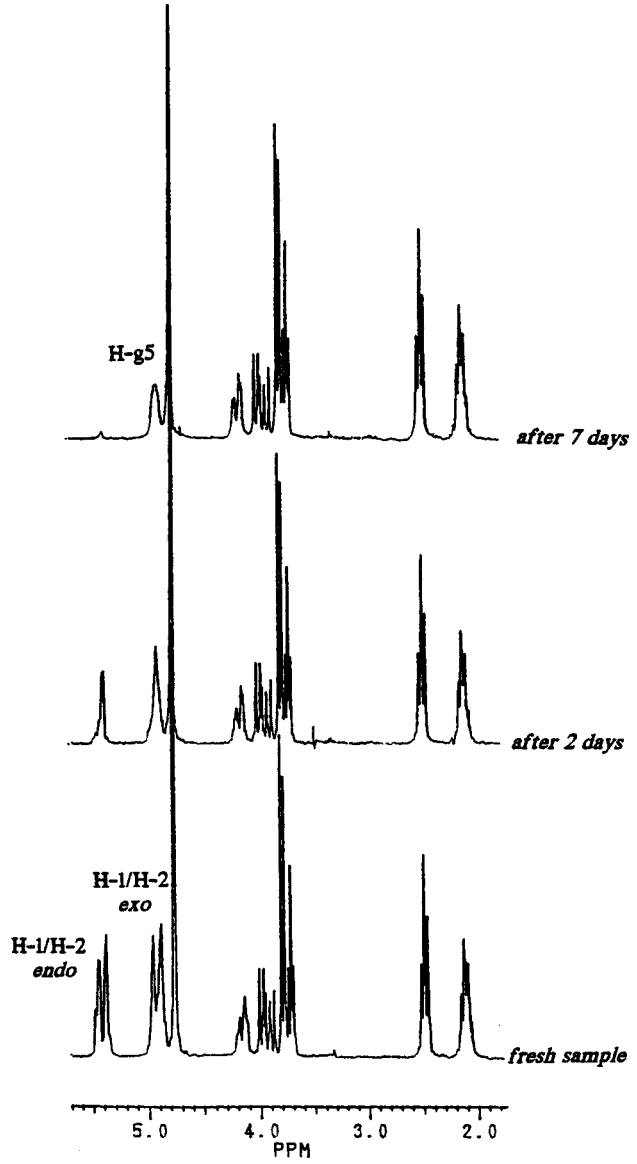

Figure 4. ^1H spectra of complex **8** (range 5.70−1.78 ppm) in D_2O (pH 6.9) at 298 K obtained at different time intervals after sample preparation. The peaks belonging to H1 and H2 protons gradually disappear due to exchange with deuterium, while the H-g5 proton—hiding under H1/H2 exo protons—emerges.

The H1 and H2 protons of the tridentate pyridinedithiol ligand in complex **8** show an interesting behavior, since in the D_2O solution, they are exchanged with deuterium and gradually disappear from the NMR spectrum (Figure 4). To confirm the process of hydrogen−deuterium exchange, we lyophilized and redissolved in H_2O the sample of **8** already in D_2O. After a week at room temperature, the H_2O was removed, and the complex redissolved in D_2O. In the ^1H spectrum, immediately after solvation, the H1 and H2 protons were again present. As a result of this exchanging process, at room temperature, carbons C1 and C2 appear as a very broad peak barely distinguishable above the noise level. These peaks completely disappear as the temperature is raised, apparently due to the increase in the rate of exchange. The activation of the carbon−hydrogen bond of C1 and C2 toward the electrophilic substitution of H1 and H2 hydrogens by deuterium can be explained by the close vicinity of the pyridinium ring that can stabilize the development of the negative charge at C1 and C2 through resonance and inductive effects. No exchange was evident between the protons

of the chelated tridentate ligand backbone and the solvent for complexes **5**, **6**, and **7**.

Thermodynamic Study of the Interaction of ReO(L^n/L) Complexes with GSH. Kinetic Aspects of the Interaction. Isothermal titration calorimetry[25] provides a technique for kinetic studies of the reaction of ReO(L^n/L) complexes with GSH. When a solution of the respective ReO(L^n/L) complex is added to a solution of GSH, heat is being absorbed, as expected for an endothermic process. The rate of heat absorption increases with time as long as the injection lasts and reaches a maximum soon after the injection is complete. It then decays exponentially to the baseline level. In the isothermal titration microcalorimetric techniques, the rate of heat flow (dQ/dt) is monitored continuously as a function of time and measured with high accuracy. From the time dependence of the heat flow, information can be extracted concerning the total heat produced by the reaction under the specific experimental conditions and the kinetic behavior of the reaction as well. The total heat (Q) is equal to the area under the curve of dQ/dt, and the change in enthalpy (ΔH) is equal to Q divided by the amount of the respective ReO(L^n/L) complex that reacted with GSH. The kinetic information is deduced directly from the dQ/dt curve, since the rate at which heat is being released or absorbed during a reaction is proportional to the rate at which the reaction products are formed.[26,27]

$$\mathrm{d}Q/\mathrm{d}t = V(\Delta H)\,\mathrm{d}P/\mathrm{d}t \qquad (1)$$

Here, V is the volume of the calorimetric cell, and P is the concentration of the reaction product. As demonstrated by Nock et al.,[10] the reaction of the ReO(L^n/L) complexes with GSH in an excess of GSH is described by pseudo-first-order rate equations:

$$C(t) = C_0 \exp(-kt) \qquad (2)$$

where $C(t)] = -P(t)$ is the concentration of the reacting ReO(L^n/L) complex, C_0 is the concentration at $t = 0$, and k is the reaction rate constant. The heat flow measured is thus given by

$$\mathrm{d}Q/\mathrm{d}t = V(\Delta H)k[C_0] \exp(-kt) \qquad (3)$$

Equation 3 indicates that calorimetric data can be used to explore kinetic aspects of the reactions under study. Indeed, it has been demonstrated that monoexponential kinetics determined by isothermal titration microcalorimetry were identical to those determined by standard spectrophotometric techniques.[26] When microcalorimetry is used for kinetic studies, the calorimetric data need to be corrected for the instrumental response time, as described previously.[28]

The calorimetric data of dQ/dt vs t from isothermal titrations of aqueous DMF GSH (1 mM) with a single 10 μL injection of an aqueous DMF (5×10^{-5} M) solution of the respective ReO(L^n/L) complexes are shown in Figure 5. Data for $t < 15$ s, when dQ/dt is increasing until it reaches maximum value (the injection lasts for 6.3 s), have been omitted from the figure, as they have also been excluded from the analysis. The data have been corrected for the instrumental relaxation time and have been analyzed via nonlinear, least-squares curve fitting to a monoexponential decaying function of the form dQ/d$t = A$ exp($-kt$), with two free parameters. The fitting results for k are summarized in Table 5. For all the data sets presented, $t = 0$ was set as the time at which the injection of the aqueous DMF solutions of the respective ReO(L^n/L) complexes began. As can be seen from the values reported in Table 5, the interaction of GSH with **2** is the fastest of the three that were studied, and the interaction with **1** is the slowest. This trend is in agreement with the trend reported previously.[10] Results for ΔH are also presented in Table 5. The ΔH values in kilocalorie per mole of the added complex follow the same trend as k. It must be noted though that these reaction enthalpies (at 37 °C) do not represent the heat absorbed for the GSH/ReO(L^n/L) reaction. They also include heat produced by the rearrangement of the solvent (DMF/water) molecules around the two reactants, which is different for the two molecules due to their solubility differences in this particular solvent. Nevertheless, the interaction of **2** with GSH has the largest ΔH values, and the interaction of **1** has the smallest.

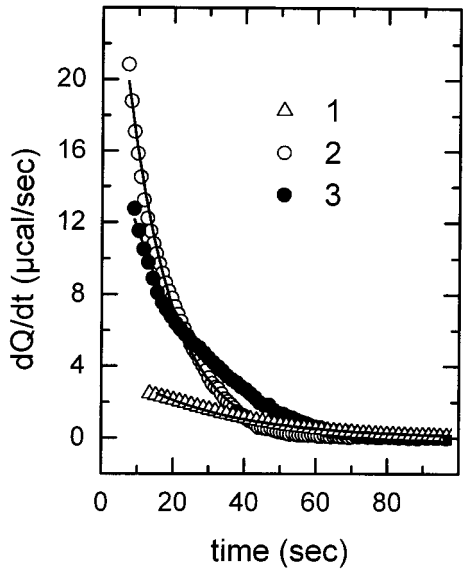

Figure 5. Rate of heat absorbed (dQ/dt) vs time for the reactions of GSH with **1**, **2**, and **3**. The lines are nonlinear least-squares fits to pseudo-first-order eq 3.

Table 5. PseudoFirst-Order Rate Constants (k) and Corresponding Enthalpy Changes (ΔH) for the Interaction of **1**, **2**, and **3** with Aqueous DMF Solutions of GSH at 37 °C

	1	**2**	**3**
k (s^{-1})	0.035 ± 0.002	0.079 ± 0.001	0.052 ± 0.001
ΔH (kcal mol^{-1})[a]	266 ± 19	716 ± 43	678 ± 40

[a] ΔH values have been scaled using the amount of the added complexes.

Conclusions

In conclusion, previous studies have demonstrated that the monothiolate coligand in MO(SNS/S) mixed-ligand complexes undergoes nucleophilic substitution with excess thiol and, in particular, with the native thiol GSH.[10,11] It was also shown that nucleophilic substitution with GSH leading to a more hydrophilic daughter species is the mechanism underlying the prolonged retention of several of the ^{99m}TcO(SNS/S) complexes in brain tissue. The rate of this conversion was found to depend primarily on the N-substituent of the central nitrogen in the SNS ligand at tracer (^{99m}Tc) level.[10] However, despite the fact that a ReO(SNS/SG) compound has been characterized, full char-

(25) Wiseman, T.; Williston, S.; Brandts, J. F.; Lin, L. N. *Anal. Biochem.* **1989**, *179*, 131−137.
(26) Morin, P. E.; Freire, E. *Biochemistry* **1991**, *30*, 8494−8500.
(27) Williams, B. A.; Toone, E. J. *J. Org. Chem.* **1993**, *58*, 3507−3510.
(28) Mayorga, O. L.; Freire, E. *Biophys. Chem.* **1987**, *87*, 87−96.

acterization of related ReO(SNS/SG) species containing SNS ligands with different pendant N-substituents has not been reported yet.[11] In addition, the impact of the pendant arm type N-positioned in the parent ReO(SNS/S) complexes on the rate of GSH substitution has, so far, not been thoroughly investigated at the macromolar level.

These issues have been addressed in the present work. Thus, four ReO(L^n/L) complexes, each carrying a different pendant group on the central nitrogen of the SNS ligand, have been synthesized and characterized. Their interactions with excess GSH and the formation of the respective daughter ReO(L^n/SG) complexes were verified by RP-HPLC on a photodiode array UV detector. The detector enabled recognition of each parent or daughter complex by its individual "footprint" on the UV spectrum. By synthesizing the ReO(L^n/SG) complexes starting from the $ReOCl_3[P(C_6H_5)_3]_2$ precursor, we obtained a more detailed characterization employing elemental analyses and several spectroscopic techniques, especially NMR. This is the first study in which ReO(SNS/SG) complexes have been produced by the direct action of GSH on the $ReOCl_3[P(C_6H_5)_3]_2$ precursor.

The influence of the N-group on the rate of conversion of ReO(L^n/L) to ReO(L^n/SG) was studied using isothermal titration microcalorimetry for complexes **1**−**3**. Complex **4** was excluded from the calorimetric measurements, since it decomposed rapidly under the applied conditions. The analysis of the calorimetric data was based on single exponential decays, since the reaction in excess amounts of GSH (1 mM: 5×10^{-5} M GSH/ReO(L^n/L)) is pseudo-first-order. The results confirm the trends reported for analogous ^{99m}Tc complexes.[10] That previous study, based on HPLC methods, provided little information for fast reactions (<1 min). The observed differences in the *k* values are attributed to several parameters that differed in the two studies, most importantly, the different solvent composition (water/DMF vs water), the ratios of reactants, and, of course, the different metal nuclides used—rhenium vs ^{99m}Tc. Complexes of the two metals in higher oxidation states often show different reaction rates during ligand-exchange processes.[29−31] In this case however, similar trends of reactivities toward GSH substitution were observed within the series of the tested rhenium and ^{99m}Tc complexes. Thus, the GSH reaction with **2** is much faster than the reaction with **1**, while **3** exhibits an intermediate reactivity.

Acknowledgment. The authors thank John Boutaris and the Agricultural Bank of Greece (ATE) for partial financial support to A. T.

Supporting Information Available: Tables of fractional atomic coordinates and thermal parameters, complete listings of bond lengths and angles, and observed and calculated structure factors. This material is available free of charge via the Internet at http://pubs.acs.org. Two CIF in ASCII format have been deposited to the Cambridge Crystallographic Data Base (CCDC 140840 and CCDC 140841).

IC000350M

(29) Deutsch, E.; Libson, K.; Jurisson, S.; Lindoy, L. *Prog. Inorg. Chem.* **1983**, *30*, 75−139.
(30) Deutsch, E.; Libson, K. *Comments Inorg. Chem.* **1984**, *3*, 83−103.
(31) Deutsch, E.; Libson, K.; Vanderheyden, J.-L.; Ketring, A. R.; Maxon, H. R. *Nucl. Med. Biol.* **1986**, *13*, 465−477.